Electronic Supplementary Material (ESI) for Dalton Transactions.
This journal is © The Royal Society of Chemistry 2022

Supporting Information

Dual-sensitized Eu(III)/Tb(III) complexes exhibiting tunable luminescent emission and application in cellular-imaging

Cui Zhang,[a#] Xiufang Ma,[b#] Peipei Cen,*[a] Huifang Yang,[a] Zixin He,[a] Yan Guo,[b] Danian Tian,*[a] and Xiangyu Liu*[bc]

[a] College of Public Health and Management, Key Laboratory of Environmental Factors and Chronic Dlsease Control, Ningxia Medical University, Yinchuan 750021, China

[b] State Key Laboratory of High-efficiency Utilization of Coal and Green Chemical Engineering, College of Chemistry and Chemical Engineering, Ningxia University, Yinchuan 750021, China

[e] State Key Laboratory of Coordination Chemistry, Nanjing University, Nanjing, 210023, China

# These authors contributed equally to this work.

***Corresponding author**

Dr. Peipei Cen

E-mail: 13895400691@163.com

***Corresponding author**

Dr. Danian Tian

E-mail: tiandanian@163.com

***Corresponding author**

Dr. Xiangyu Liu

E-mail: xiangyuliu432@126.com

Contents:

Cell viability assay in dark (CCK-8 assay)

CCK-8 assay was carried out to evaluate the cytotoxicity or cell viability of **1** and **2**: HeLa (immortal cervical cancer cell line) and MCF-7 (breast cancer cell line) cells were plated in 96-well plates (10^4 cells per well) and incubated for 24 h with complexes **1**/**2** at a wide concentration range from 0 μg/mL to l00 μg/mL. Each concentration was tested in 6 wells. About 24 h after incubation, each well was washed with Dulbecco's phosphate buffered saline, and then 100 μL of DMEM and 10 μL of CCK-8 solution were add after incubation for another 1h. The optical density (OD) was measured at 450 nm with a microtiter plate reader. The cell viability was calculated using the following equation:

$$\text{Viable cells (\%)} = \frac{OD_{sam} - OD_{bla}}{OD_{con} - OD_{bla}} * 100\%$$

OD_{sam} was obtained with the prepared complex **1**/**2**; OD_{con} was obtained without the complex **1**/**2**. OD_{bla} was contained without the complex and no cells. The optical density of absorbance is directly proportional to the number of live cells. All the in vitro cytotoxicity experiments were performed in triplicate. All the values for % cell proliferation was normalized with respect to untreated cells and a graph was plotted between % cell viability and concentration of complexes **1** and **2**.

Table S1. Crystal Data and Structure Refinement Details for complexes **1** and **2.**

	1	**2**
Empirical formula	$C_{44}H_{26}EuF_9N_4O_6$	$C_{44}H_{26}TbF_9N_4O_6$
Formula weight	1029.65	1036.61
Crystal system	monoclinic	monoclinic
Space group	$P2_1/c$	$P2_1/c$
a (Å)	11.0774(10)	10.9811(3)
b (Å)	27.429(2)	27.1423(8)
c (Å)	28.137(3)	27.9453(5)
α (°)	90	90
β (°)	93.525(3)	93.546(2)
γ (°)	90	90
V (Å^3)	8533.1(13)	8313.2(4)
Z	8	8
μ (mm^{-1})	1.562	9.207
Unique reflections	19572	14523
Observed reflections	185259	27012
R_{int}	0.0484	0.0397
Final R indices [$I>2\sigma(I)$]	$R_1 = 0.0494$	$R_1 = 0.0657$
	$wR_2 = 0.1081$	$wR_2 = 0.1532$
R indices (all data)	$R_1 = 0.0696$	$R_1 = 0.0419$
	$wR_2 = 0.1167$	$wR_2 = 0.0643$

Table S2. Selected bond lengths (Å) and bond angles (°) for complexes **1** and **2.**

Complex **1**			
Eu(1)-O(1)	2.344(4)	O(4)-Eu(1)-O(2)	73.70(11)
Eu (1)-O(2)	2.389(3)	O(4)-Eu(1)-N(1)	128.71(12)
Eu (1)-O(3)	2.368(3)	O(4)-Eu(1)-N(2)	77.00(12)
Eu (1)-O(4)	2.381(3)	O(5)-Eu(1)-O(2)	131.80(13)
Eu (1)-O(5)	2.345(3)	O(5)-Eu(1)-O(3)	77.53(13)
Eu (1)-O(6)	2.340(3)	O(5)-Eu(1)-O(4)	134.01(12)
Eu (1)-N(1)	2.615(4)	O(5)-Eu(1)-N(1)	76.93(12)
Eu(1)-N(2)	2.590(4)	O(5)-Eu(1)-N(2)	139.46(12)
Eu(2)-O(7)	2.385(3)	O(6)-Eu(1)-O(1)	101.25(14)
Eu(2)-O(8)	2.336(4)	O(6)-Eu(1)-O(2)	84.15(11)
Eu(2)-O(9)	2.361(3)	O(6)-Eu(1)-O(3)	89.70(12)
Eu(2)-O(10)	2.355(3)	O(6)-Eu(1)-O(4)	75.39(11)
Eu(2)-O(11)	2.378(3)	O(6)-Eu(1)-O(5)	71.53(11)
Eu(2)-O(12)	2.364(3)	O(6)-Eu(1)-N(1)	148.41(12)
Eu(2)-N(5)	2.608(4)	O(6)-Eu(1)-N(2)	148.89(12)
Eu(2)-N(6)	2.592(4)	N(2)-Eu(1)-N(1)	62.55(12)
O(1)-Eu(1)-O(2)	70.10(13)	O(7)-Eu(2)-N(5)	77.64(12)
O(1)-Eu(1)-O(3)	144.87(13)	O(7)-Eu(2)-N(6)	139.78(12)
O(1)-Eu(1)-O(4)	143.80(13)	O(8)-Eu(2)-O(7)	70.98(12)
O(1)-Eu(1)-O(5)	74.65(15)	O(8)-Eu(2)-O(9)	82.28(13)
O(1)-Eu(1)-N(1)	71.52(14)	O(8)-Eu(2)-O(10)	93.00(14)
O(1)-Eu(1)-N(2)	92.62(15)	O(8)-Eu(2)-O(11)	76.03(14)
O(2)-Eu(1)-N(1)	119.56(12)	O(8)-Eu(2)-O(12)	93.79(13)
O(2)-Eu(1)-N(2)	74.53(12)	O(8)-Eu(2)-N(5)	148.59(12)
O(3)-Eu(1)-O(2)	144.79(11)	O(8)-Eu(2)-N(6)	148.71(12)
O(3)-Eu(1)-O(4)	71.20(11)	O(9)-Eu(2)-O(7)	134.07(13)
O(3)-Eu(1)-N(1)	81.68(12)	O(9)-Eu(2)-O(11)	74.23(12)
O(3)-Eu(1)-N(2)	94.78(13)	O(9)-Eu(2)-O(12)	145.05(12)
Complex **2**			
Tb(1)-O(7)	2.342(6)	O(10)-Tb(1)-O(7)	75.3(2)
Tb(1)-O(8)	2.332(5)	O(10)-Tb(1)-O(8)	94.3(2)
Tb(1)-O(9)	2.353(6)	O(10)-Tb(1)-O(9)	71.8(2)
Tb(1)-O(10)	2.309(6)	O(10)-Tb(1)-O(11)	81.2(2)
Tb(1)-O(11)	2.335(5)	O(10)-Tb(1)-O(12)	93.4(2)
Tb(1)-O(12)	2.330(5)	O(10)-Tb(1)-N(1)	148.9(2)
Tb(1)-N(1)	2.582(6)	O(10)-Tb(1)-N(2)	148.0(2)
Tb(1)-N(2)	2.559(7)	O(1)-Tb(2)-O(2)	70.8(2)
Tb(2)-O(1)	2.316(7)	O(1)-Tb(2)-O(3)	144.3(2)
Tb(2)-O(2)	2.368(6)	O(1)-Tb(2)-O(4)	144.0(2)

Tb(2)-O(3)	2.338(6)	O(1)-Tb(2)-O(5)	74.0(3)
Tb(2)-O(4)	2.349(6)	O(1)-Tb(2)-N(1)	71.7(2)
Tb(2)-O(5)	2.320(6)	O(1)-Tb(2)-N(2)	93.1(3)
Tb(2)-O(6)	2.302(5)	O(2)-Tb(2)-N(1)	121.1(2)
Tb(2)-N(1)	2.585(7)	O(2)-Tb(2)-N(2)	75.0(2)
Tb(2)-N(2)	2.552(7)	O(3)-Tb(2)-O(2)	144.7(2)
O(7)-Tb(1)-O(9)	130.4(2)	O(3)-Tb(2)-O(4)	71.6(2)
O(7)-Tb(1)-N(1)	128.9(2)	O(3)-Tb(2)-N(1)	81.0(2)
O(7)-Tb(1)-N(2)	76.8(2)	O(3)-Tb(2)-N(2)	94.9(2)
O(8)-Tb(1)-O(7)	71.9(2)	O(4)-Tb(2)-O(2)	73.2(2)
O(8)-Tb(1)-O(9)	74.7(2)	O(4)-Tb(2)-N(1)	128.8(2)
O(8)-Tb(1)-O(11)	145.0(2)	O(4)-Tb(2)-N(2)	76.5(2)
O(8)-Tb(1)-N(1)	78.74(19)	O(5)-Tb(2)-O(2)	131.7(2)
O(8)-Tb(1)-N(2)	91.7(2)	O(5)-Tb(2)-O(3)	77.4(2)
O(8)-Tb(1)-N(1)	77.2(2)	O(5)-Tb(2)-N(1)	75.9(2)
O(8)-Tb(1)-N(2)	139.9(2)	O(5)-Tb(2)-N(2)	139.4(2)

Table S3. Ln (III) ions geometry analysis of **1** and **2** by SHAPE 2.1 software.

Configuration	ABOXIY, **1(Eu1)**	ABOXIY, **1(Eu2)**	ABOXIY, **2(Tb1)**	ABOXIY, **2(Tb2)**
Hexagonal bipyramid (D_{6h})	15.442	15.767	15.813	15.456
Cube (O_h)	9.759	9.562,	9.487	9.805
Square antiprism (D_{4d})	3.025	2.435	2.427	2.856
Triangular dodecahedron (D_{2d})	0.609	0.634	0.554	0.570
Johnson gyrobifastigium J26 (D_{2d})	14.094	14.261	14.253	13.949
Johnson elongated triangular bipyramid J14 (D_{3h})	29.217	30.018	29.981	29.326
Biaugmented trigonal prism J50 (C_{2v})	3.278	2.650	2.692	3.081
Biaugmented trigonal prism (C_{2v})	2.672	1.845	1.864	2.603
Snub siphenoid J84 (D_{2d})	3.131	3.209	3.118	3.000
Triakis tetrahedron(T_d)	10.456	10.261	10.225	10.503
Elongated trigonal bipyramid(D_{3h})	23.683	25.138	25.138	23.828

Table S4. Photophysical properties for the reported analogous lanthanide complexes.

complexes	$\tau_{everage}$(μs)	φ(%)	reference
$Eu(acac)_3(PyAm)$	514±1	3±0.8	1
$Tb(acac)_3(PyAm)$	826±0.8	65±3	1
$Eu(hfaa)_3(Py\text{-}Im)$	833.01	74.36	2
$Eu(hfa)_3(DPCO)_2$	6.5×10^5	73	3
$Eu(hfa)_3(TPPO)_2$(Solid)	8.0×10^5	51	3
$Eu(hfa)_3$((R)-bidp)	690	76	4
$Eu(TCPB)_3Phen$	830	59	5
$Eu(TMHD)_3Phen$	760	61	5
$Tb(tmh)_3(PEB)$	1200	71	6
$Tb_2(tmh)_6$(m-BPEB)	810	39	6
$Eu(hfa)_3(dpt)$	750	75	7
$Eu(hfa)_3(dpbp)$	850	72	7
$Eu(hfa)_3(dpedtt)$	740	73	8
$Eu(hfa)_3(dpedot)$	930	85	8
$Eu(acac)_3(Br_2\text{-}phen)$	790±1.53	13	9
$Eu(hfa)_3(TPPO)_2(CDCl_3)$	790±0.93	72	10
$Eu(hfa)_3(DPPTO)_2$	790±1.4	76	10
$Eu(dpq)(tfnb)_3$	857(H_2O)/1597(D_2O)	19.9	11
$Tb(dpq)(tfnb)_3$	403(H_2O)/437(D_2O)	15.5	11

acac: acetylacetonate; PyAm2-amidinopyridine; Py-Im: 2-(2-pyridyl) benzimidazole; Hfaa: hexafluoroacetylacetone; DPCO: diphenylphosphorylchrysene; TPPO: triphenylphosphine oxide; Phen: mono-(1,10-phenanthroline); TCPB: tris-(4,4,4-trifluoro-1-chlorophenyl-butane- dione; PEB: (diphenylphosphoryl) ethynyl) benzene; TMHD: tris-(2,2,6,6-tetramethyl-heptanedione); tmh: 2,2,6,6-tetramethyl-3,5-heptanedione; Br_2-phen: 4,7-dibromo-1,10-phenanthroline; m-BPEB: 1,3-bis(diphenylphosphoryl) ethynyl) benzene; hfa: hexauoroacetylacetonate; dpt: 2,5-bis(diphenylphosphoryl)thiophene; dpbp: 4,4'-bis(diphenylphosphoryl) biphenyl; dpedtt: 2,5-bis(diphenylphosphoryl) -3,4-ethylenedi- thiothiophene; dpedot:2,5-bis(diphenylphosphoryl) -3,4-ethylenedi-oxythiophene; (R)-bidp: (R)-1,1'-binaphthyl-2,2'-bis-(diphenylphosphinate); DPPTO: 2-diphenylphosphoryltri-phenylene; dpq: dipyrido(3,2-d:2',3'-f)quinoxaline; tfnb: 4,4,4-trifluoro-1-(2-napthyl)-1,3-butanedione.

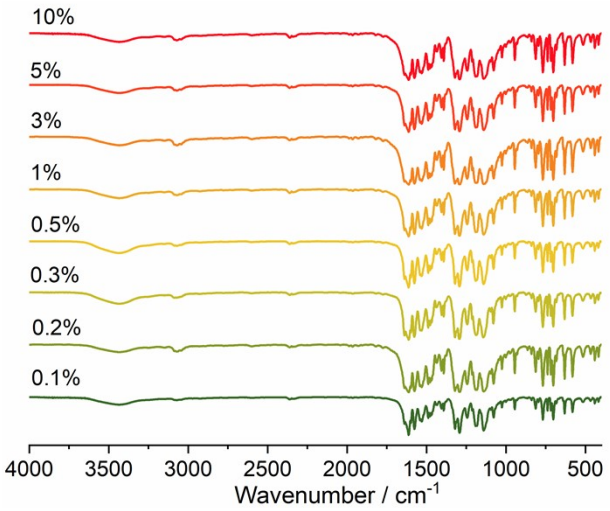

Figure S1. IR curves of $\mathbf{Eu_xTb_{1-x}}$ (x = 0.1%-10%).

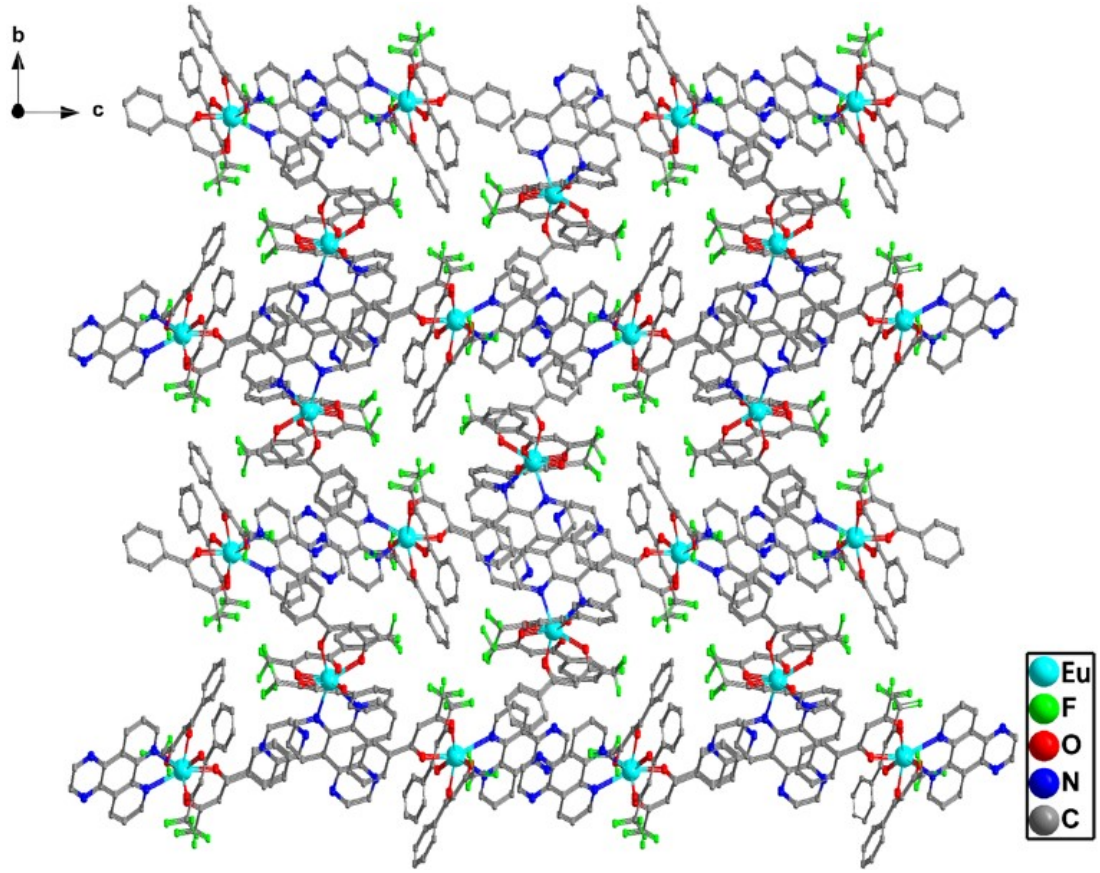

Figure S2. Molecular stacking charts of complexes **1**. All hydrogen atoms are omitted for clarity.

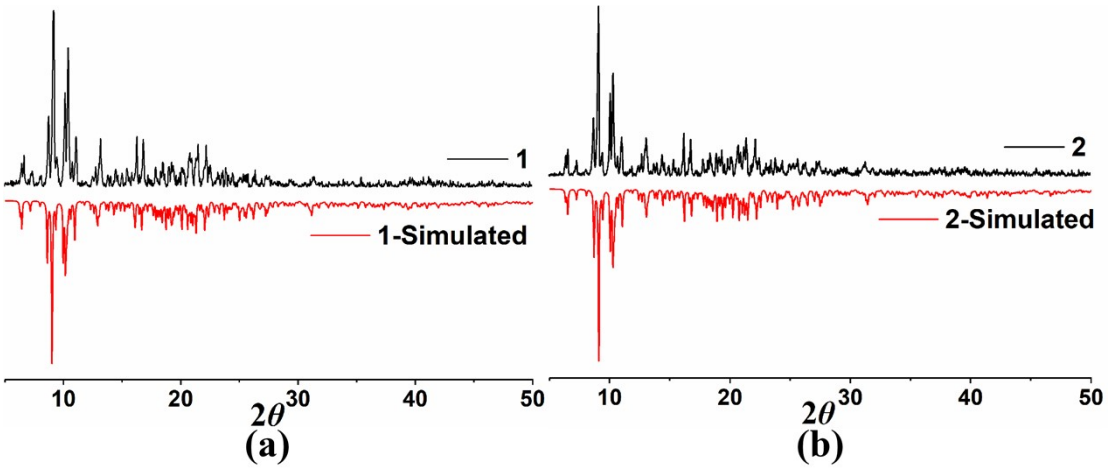

Figure S3. PXRD curves of **1** (a) and **2** (b).

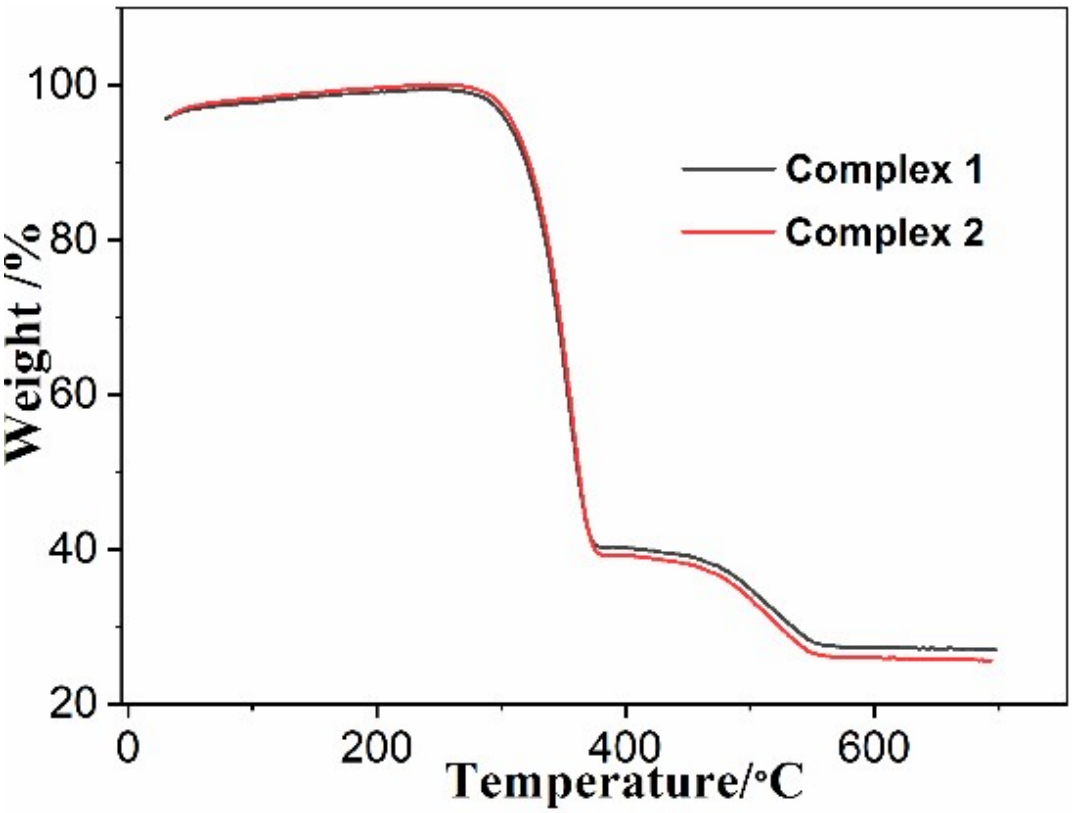

Figure S4. TGA plots of **1** and **2** under N_2 environment.

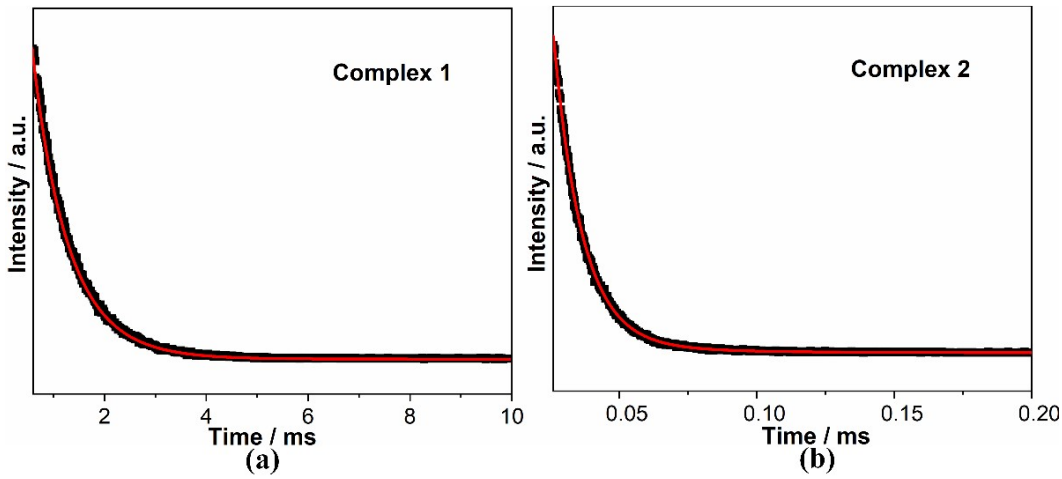

Figure S5. Fluorescence decay curve from $^5D_0$ and $^5D_4$ states and lifetime measurements at 613 nm and 545 nm for Eu^{3+} and Tb^{3+} in complexes **1** and **2** (a and b) respectively (λ_{ex} = 348 nm for complex **1** and λ_{ex} = 362 nm for complex **2**). The red curves are the best fits considering two exponential behavior of the decay.

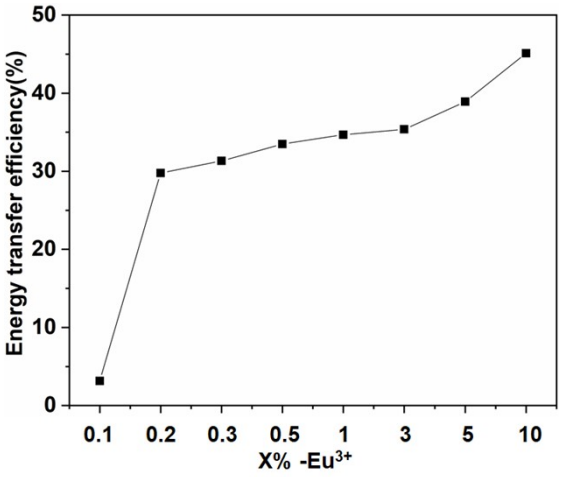

Figure S6. The energy transfer efficiency from Tb^{3+} to Eu^{3+} in $\mathbf{Eu_xTb_{1-x}}$.

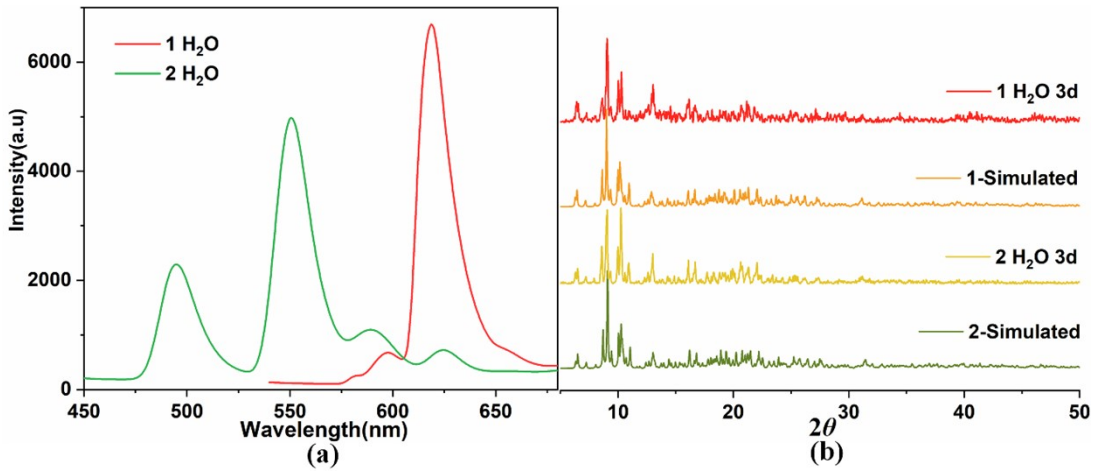

Figure S7. (a) luminescence spectra of **1** and **2** in aqueous solution; (b) PXRD patterns of **1** and **2** immersed in aqueous solution for 3 days.

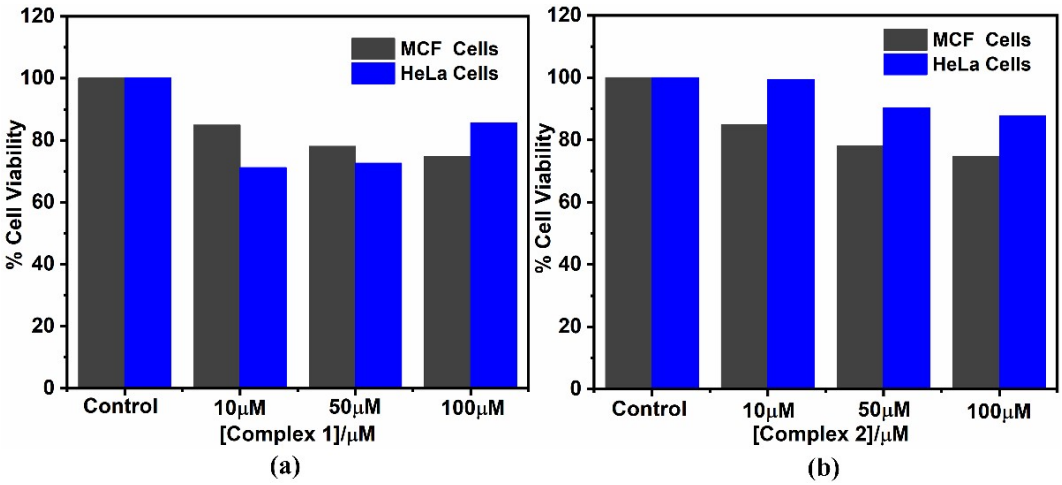

Figure S8. Cell viability plots showing the cytotoxicity of **1**(a) and **2**(b) with HeLa and MCF-7 cells on 24 h incubation by CCK-8 assay.

Reference

1 A. A. Kitos, D. A. Gálico, R. Castañeda, J. S. Ovens, M. Murugesu and J. L. Brusso. Stark Sublevel-Based Thermometry with Tb(III) and Dy(III) Complexes Cosensitized via the 2-Amidinopyridine Ligand . *Inorg. Chem*., 2020, **59**, 11061-11070.

2 R. Ilmi, M. S. Khan, Z. Li, L. Zhou, W. Y. Wong, F. Marken and P. R. Raithby. Utilization of ternary europium complex for organic electroluminescent devices and as a sensitizer to improve electroluminescence of red-emitting iridium complex. *Inorg. Chem*., 2019, **58**, 8316-8331.

3 Y. Kitagawa, M. Kumagai, T. Nakanishi, K. Fushimi and Y. Hasegawa. The Role of π–f Orbital Interactions in Eu (III) Complexes for an Effective Molecular Luminescent Thermometer. *Inorg. Chem*., 2020, **59**, 5865-5871.

4 N. Koiso, Y. Kitagawa, T. Nakanishi, FK. Ushimi and Y. Hasegawa. Eu (III) chiral coordination polymer with a structural transformation system. *Inorg. Chem*., 2017, **56**, 5741-5747.

5 O. T. Alexander, R. E. Kroon, A. Brink and H. G.Visser. Symmetry correlations between crystallographic and photoluminescence study of ternary β-diketone europium (III) based complexes using 1, 10-phenanthroline as the ancillary ligand. *Dalton Trans.*, 2019, **48**, 16074-16082.

6 P. P. Ferreira da Rosa, T. Nakanishi, Y. Kitagawa, T. Seki, H. Ito, K. Fushimi and Y. Hasegawa. Thermosensitive Seven-Coordinate Tb-III Complexes with LLCT Transitions. *Chem. Eur. J*., 2018, **19**, 2031-2037.

7 Y. Hirai, T. Nakanishi, Y. Kitagawa, K. Fushimi, T. Seki, H. Ito and Y. Hasegawa. Luminescent Europium (III) Coordination Zippers Linked with Thiophene-Based Bridges. *Angew. Chem. Int. Ed*., 2016, **55**, 12059-12062.

8 Y. Hirai, P. P. Ferreira da Rosa, Y. Kitagawa and Y. Hasegawa. Thermal and Crystallographic Investigation of Luminescent Eu (III) Coordination Polymers with Dithiane and Dioxane Hexyl Rings. *Chem. Lett.*, 2019, **48**, 1544-1546.

9 R. Ilmi, S. Kansız, N. Dege and M. S. Khan.Synthesis, structure, Hirshfeld surface analysis and photophysical studies of red emitting europium acetylacetonate complex incorporating a phenanthroline derivative. *J. PHOTOCH. PHOTOBIO. A.,* 2019, **377**, 268-281.

10 Y. Kitagawa, F. Suzue, T. Nakanishi, K. Fushimi and Y. Hasegawa. A highly luminescent Eu (III) complex based on an electronically isolated aromatic ring system with ultralong lifetime. *Dalton Trans.*, 2018, **47**, 7327-7332.

11 S. Dasari, S. Singh, S. Sivakumar and A. K. Patra. Dual-sensitized luminescent europium (III) and terbium (III) complexes as bioimaging and light-responsive therapeutic agents. *Chem. Eur. J.*,2016, **22**, 17387-17396.